Indian Journal of Fundamental and Applied Life Sciences ISSN: 2231-6345 (Online)
An Open Access, Online International Journal Available at http://www.cibtech.org/jls.htm
2015 Vol. 5 (2) April-June, pp.28-33/Afroozeh et al.
Research Article

DEVELOPMENT OF SPINNING TECHNIQUE ON THE FIBER MORPHOLOGY

[*]Abdolkarim Afroozeh[1,2], Alireza Zeinalinezhad[3] and Narges Hashem Nazari[2]
[1]Young Researchers and Elite Club, Jahrom Branch, Islamic Azad University, Jahrom, Iran
[2]The Department General of Fars Province Education, Iran
[3]Department of Chemistry, Anar Branch, Islamic Azad University, Anar, Iran
**Author for Correspondence*

ABSTRACT
In this study the influence of spinning technique on the fiber morphology and micro-structures, a novel processing method was developed. In order to implement this new approach this study focuses on the optimization of several processing parameters including gelation, coagulation, polymer content, filler loading, flow, and heat treatment.
.

Keywords: *Fiber Morphology, Polymer, Carbon Nanochip*

INTRODUCTION
Fiber spinning can induce alignment of either polymer chains or nano-fillers in composites (Xie *et al.*, 2005; Ning *et al.*, 2012). It has been found that the degree of orientation and crystalline formations for fiber components are also dependent on the shear rates (Yamamoto *et al.*, 2015; Sun *et al.*, 2015). Control of the applied shear stress and rates is also important for the final fiber morphology (Needleman, 2015; Abdullah *et al.*, 2015). For example, variations of the shear rates perpendicular to the fiber axis caused by the mold geometry or liquid flow-field can induce skin-core structures (Chen *et al.*, 2015; Agassant and Mackley, 2015). In such cases, higher shear rates together with increased solidification/cooling rates near the fiber surface leads to higher alignment near the fiber surface, while the interior alignment remains more isotropic (Silva *et al.*, 2015; Fan, 2015; Afroozeh *et al.*,). This leads to a non-uniform fiber microstructure. Based on the anisotropic character of the fiber it is clear that maximizing the highly oriented portion will have a major contribution to the fiber property (Li *et al.*, 2015; Abdellaoui *et al.*, 2015; Afroozeh *et al.*, 2015). In this study a laminar flow-field is coupled with gel-spinning to produce fibers with increased orientation/alignment of both the polymer and nC components, decreased fiber diameter and induced fibrillar crystallization during spinning (Ram *et al.*, 2015; Wang *et al.*, 2015).

MATERIALS AND METHODS
Methedology
Here the flattened FWNT with average aspect ratio ~10, consisting of six to eight walls as-produced, nano-chips stack to form nano-fibers has shown in Figure.1. CNC were purchased from Catalytic Materials LLC Inc by width ~50 nm, average length ~500 nm, purity > 99 wt%, density ~2.2 $g \cdot cm^{-3}$, and surface area ~120 $m^2 \cdot g^{-1}$, has shown in Figures 2 to 4.

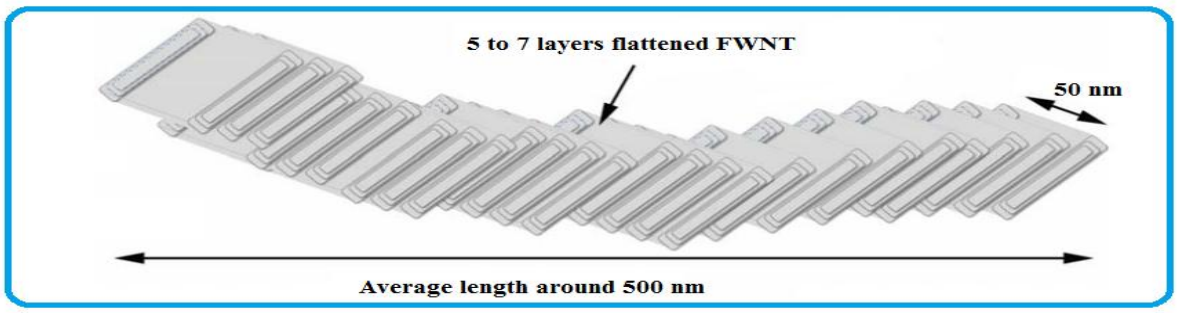

Figure 1: Schematic of carbon nanochip fiber (CNCF)

For composites, nCs of various morphologies were used for comparisons that it has shown in Figure 3.2a. Carbon nano-tubes (CNT) with bulk density 0.12 g·cm-3, average length ~1 μm, and purity 93.5 to 98.9% were purchased from Continental Carbon Nanotechnologies that shown in Figure 3.2b. Raman curve showed G/D ratio to be 20 indicating a quality in the graphitic structure. Carbon nano-spheres (CNS) are chains of interconnected spherical carbon structures exhibiting onion layers that are shown in Figure 3.2c. The CNS globular structure is examined by SEM and shows a size range from 50-90 nanometers for diameter. The CNS also exhibits a high degradation temperature of 780 °C in air. The materials are 99% pure carbon, hydrogen free, and with no embedded metals or other impurities. CNS was provided from Clean Technology International Corporation. SEM images of the nC morphologies are shown in Figure 3.2. All the materials were used as-received without further modification.

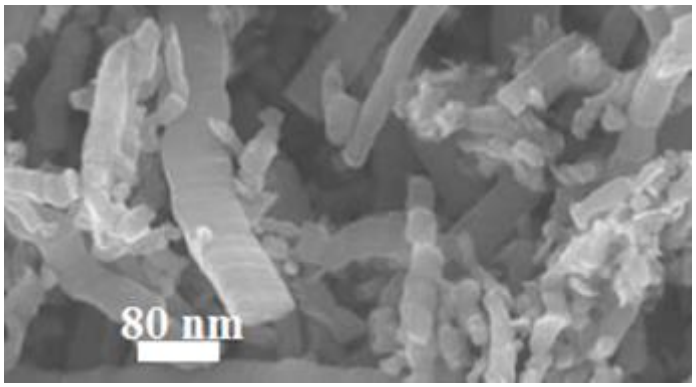

Figure 2: Various nCs, that CNC with stacked platelets morphology

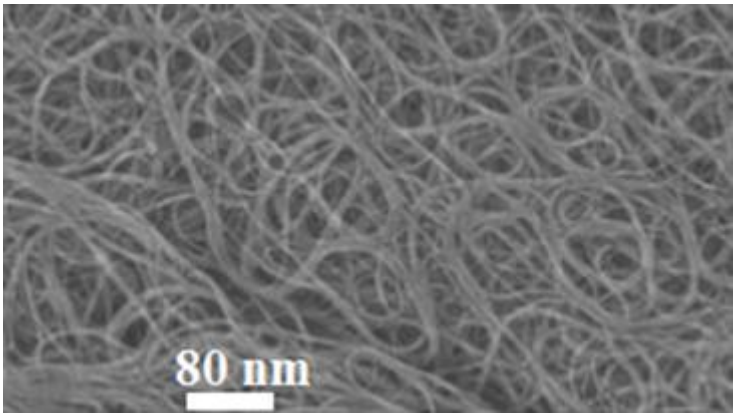

Figure 3: Various nCs, that CNT showing bundles

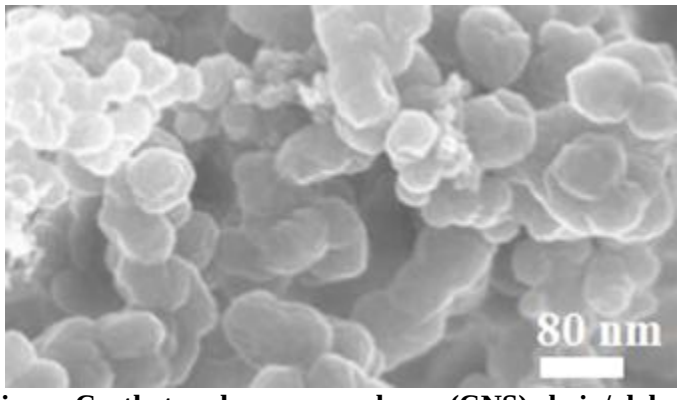

Figure 4: Various nCs, that carbon nano-spheres (CNS) chain/globular structures

The control PVA solution dopes were made by dissolving PVA into DMSO at a solution temperature of ~80 °C at various concentrations (i.e., 4, 6, 8, 10, 12, and 18 wt%). For the composite dopes the CNC were dispersed in dilute PVA solutions (concentration 2 wt%) using sonication and centrifugation for specific time i.e: 30, 50, 80 and 120 min respectively Subsequently, additional PVA is added to the dispersion to produce a dope concentration sufficient for spinning a fiber. The final CNC loadings in the dopes were 0, 0.2, 0.3, 0.4, and 2 wt%, respectively. The spinning set-up is shown in Figure 5. A solvent reservoir is used to supply and recycles the coagulant solvent, which is pumped into the connected glass tube or lower temperatures for spinning. A syringe pump is used to introduce the control and composite dopes into the glass tube. The dope is contained in a 5 ml stainless steel syringe by inside diameter 12 mm. The syringe was connected to a blunt-tip needle. The as-spun fibers are formed as soon as the dope is introduced to the flowing methanol. The glass tube length by 3 m is chosen to ensure sufficient coagulation time and fiber extension. As-spun fibers were collected on the take-up rollers. The collected fibers are further coagulated in methanol for 30 min and subsequently post-processed by heat-drawing on a hot-plate (10 inches by 1 inch) or/and annealing procedures.

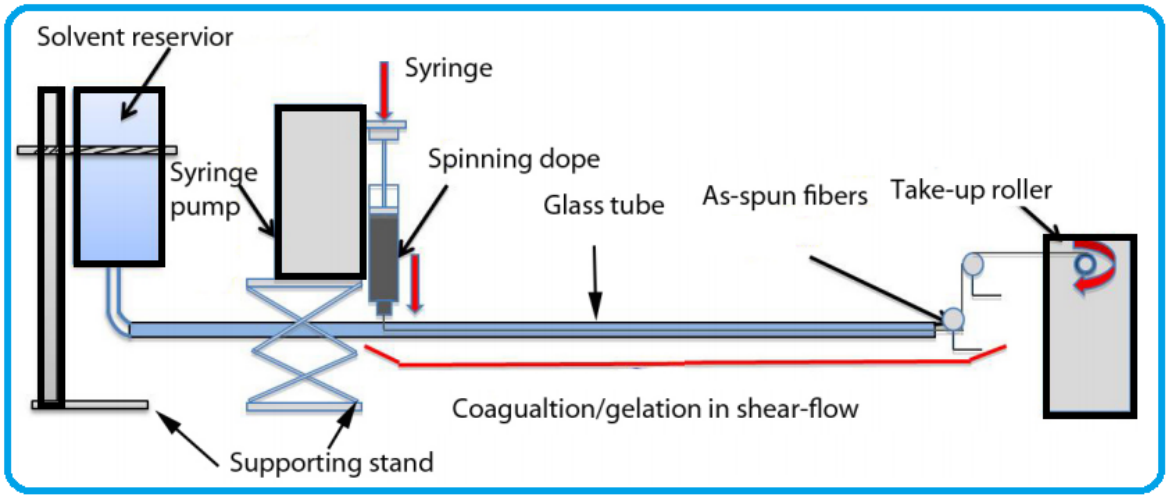

Figure 5: Schematic of flow spinning set-up

SEM and TEM were used to observe the fiber fracture surface, fiber microstructure, and nC morphology in the pre-processed or final dope solutions. Wide-angle X-ray diffraction (WAXD) and small-angle X-ray scattering (SAXS) was performed using a S-MAX3000+ 007 HFM WAXS/SAXS system that operated at 1.4 kW with a beam focal size of 40 µm, equipped with a 80 mm multi-wire 2D detector on fiber bundles. Tensile tests were conducted with 25 mm gauge at 0.08 mm·min^{-1} extension rate using a dynamic mechanical analyzer. Differential scanning calorimetry by Instruments tests were performed from 50 °C to 400 °C at a heating rate of 18 °C/min. Thermal gravimetric analysis (TGA) were done at heating rates of 24 °C·min^{-1} under air-flow from 26 °C to 800 °C to measure thermal-mechanical properties.

RESULTS AND DISCUSSION

For most semi-crystalline polymers used in wet-spinning and gel-spinning methods, the spinning dope will solidify into a fiber in the coagulation bath through the formation of physical intermolecular bonds between chains. This process is typically referred to as gelation. This gelation process is caused by exchange between the solvent and coagulant. The coagulant is a non-solvent for the polymer. For this reason, during diffusion exchange of the solvents the polymer chains form entanglements and physical linkages and gel. Gelation can be tailored by temperature variations of the dope and coagulant, polymer concentration variation in the dope, as well as coagulation time.

One factor influencing gelation process is coagulant temperature. In order to understand the polymers' gelation capability, several control PVA gel films were made at various polymer concentration and coagulant temperatures to examine the average gelation time (Table 1). The gel films were formed by injecting PVA solution droplets between glass slides followed by soaking in methanol. The gelled films formed at different time periods as a function of coagulant temperature. The gel film formation time-temperature relationships were examined for polymer concentrations ranging from 4 wt% to 15 wt%. There is a clear trend that as with lower temperature and higher polymer concentration, the coagulation time is decreased.

Table 1: PVA gel-film formation time (hrs) at various coagulant temperatures

PVA Concentration	RT	0 ° C	-20ºC	-50 ºC	-65 ºC	-75 ºC
4	11	10	9	6	2	0.5
6	6	5	3	2	1	0.8
8	1	3	1	0.7	0.5	0.2
10	0.5	0.4	0.4	0.3	0.2	0.02
12	0.3	0.2	0.1	0.04	0.03	0.02
16	0.2	0.1	0.05	0.02	0.01	0.01

As discussed, another factor affecting the gelation process is the polymer concentration. This factor is related to the spinning dope viscosity and polymer chain conformation capability in the solvent. For the PVA grade used in this work, it was found that gelation is instantaneous for a range of coagulation temperatures once the concentration increases above 15 wt .%. During the coagulation process, solvent and coagulant exchanges and the polymer chains condense to form fibers. The polymeric concentration has to be high enough when the chains are capable of forming entanglements and interactions with one another. It was found that at concentrations below 6 wt% as soon as the dope is injected into the coagulant, a fiber is formed .

However, it is unable to keep this form due to the coagulant flow caused break-up (i.e., gelled beads and discontinuous fibers). Therefore a polymer concentration between 6 wt% and 15 wt % was studied to optimize the final fiber structural quality and properties (Table 2). It has been found that the highest mechanical properties appear at the PVA concentration of 10 wt%, with modulus eached 32 GPa and tensile strength of 0.9 GPa, respectively. As-spun collection rates also show some potential for controlling the morphology and properties in the fibers. The collection rates are dependent on the injection rates, as shown in Table 2, where at low concentrations of PVA, higher injection rates are necessary to form gel fibers.

Table 2: Dependency of PVA concentration on resultant mechanical properties

Concentration	Dop Injection(ml/mim)	Take up Speed (m/min)	Draw ratio	Fiber diameter (µm)	E(GPa)	Ϭ(GPa)	ε(%)
6	0.5	20	10	8	17	0.5	10
8	0.6	21	12	9	24	0.6	5
10	0.5	22	14	8	30	0.9	5
12	0.3	10	16	13	29	0.8	5
18	0.2	9	12	20	21	0.7	5

In addition, as-spun collection rates may show some potential for controlling the morphology and properties in the fibers. The collection rates are dependent on the injection rates, as shown in Table 2. At low concentrations of PVA, higher injection rates are necessary to form gel fibers. As the fibers formed at low density, the shear flow may stretch it more than those of more highly packed fibers, therefore a higher

collection rates are needed. For this reason, lower injection rates and also smaller collection rates were observed in Table 2.

Conclusion

A flow assisted gel-spinning method was used to fabricate both the control and the composite fibers. Various spinning parameters were studied to optimize this fiber fabrication method. It was determined that as the coagulant temperature decreased, gelation time was shortened. PVA dope concentrations were also studied for its effect on the resultant fiber mechanical properties, and a 10 wt% spinning dope was found to be optimal. It was also confirmed that introducing a flow-field during coagulation caused higher polymer chain alignment and decreased fiber diameter. Coagulation temperature also influenced the as-spun fiber orientation factor, where 0 °C showed most beneficial impact. Fiber collection rates and hot-drawing procedures at various temperatures and pulling force were also found to be important toward fine-tuning the fiber microstructure. For composite fibers, dispersion optimization studies as well as the effects of composite dope loadings were performed with CNC.

REFERENCES

Abdellaoui H, Bensalah H, Echaabi J, Bouhfid R and Qaiss A (2015). Fabrication, characterization and modelling of laminated composites based on woven jute fibres reinforced epoxy resin. *Materials & Design* **68** 104-113.

Abdullah SZ, Wray HE, Bérubé PR and Andrews RC (2015). Distribution of surface shear stress for a densely packed submerged hollow fiber membrane system. *Desalination* **357** 117-120.

Afroozeh A, Arefi E, Pourmand S and Zeinalinezhad A (No Date). Secured Communication Generation Using Optical Soliton Pulse.

Afroozeh A, Mosalanezhad R, Pourmand SE and Zeinalinezhad A (2015). *Wireless Terahertz Generation Using Optical Waveguides* (American Academic Press).

Agassant JF and Mackley MR (2015). A personal perspective on the use of modelling simulation for polymer melt processing. *International Polymer Processing* **30** 121-140.

Chen Y, Fang D, Lei J, Li L, Hsiao BS and Li ZM (2015). Shear-induced precursor relaxation-dependent growth dynamics and lamellar orientation of β-crystals in β-nucleated isotactic polypropylene. *The Journal of Physical Chemistry B*.

Fan Y (2015). *Low-Cost Polymer-Based Microfluidic Systems*.

Li J, Jafarpoor M, Bouxsein M and Rutkove SB (2015). Distinguishing neuromuscular disorders based on the passive electrical material properties of muscle. *Muscle & Nerve* **51** 49-55.

Needleman A (2015). The effect of rate dependence on localization of deformation and failure in softening solids. *Journal of Applied Mechanics* **82** 021002.

Ning N, Fu S, Zhang W, Chen F, Wang K, Deng H, Zhang Q and Fu Q (2012). Realizing the enhancement of interfacial interaction in semicrystalline polymer/filler composites via interfacial crystallization. *Progress In Polymer Science* **37** 1425-1455.

Ram R, Rahaman M and Khastgir D (2015). Electrical properties of polyvinylidene fluoride (pvdf)/multi-walled carbon nanotube (mwcnt) semi-transparent composites: modelling of dc conductivity. *Composites Part A: Applied Science And Manufacturing* **69** 30-39.

Silva BL, Spinelli JE, Canté MV, Bertelli F, Cheung N, Riva R and Garcia A (2015). Experimental and numerical analyses of laser remelted sn–0.7 wt% cu solder surfaces. *Journal of Materials Science: Materials in Electronics* **26** 3100-3107.

Sun L, Chen JY, Jiang W and Lynch V (2015). Crystalline characteristics of cellulose fiber and film regenerated from ionic liquid solution. *Carbohydrate Polymers* **118** 150-155.

Wang ZJ, Weinberg G, Zhang Q, Lunkenbein T, Klein-Hoffmann A, Kurnatowska M, Plodinec M, Li Q, Chi L and Schloegl R (2015). Direct observation of graphene growth and associated copper substrate dynamics by in-situ scanning electron microscopy. *Acs Nano*.

Xie XL, Mai YW and Zhou XP (2005). Dispersion and alignment of carbon nanotubes in polymer matrix: a review. *Materials Science And Engineering: R: Reports* **49** 89-112.

Yamamoto H, Sakamoto N, Fujita A, Harada M and Ochi M (2015). Toughening mechanism of liquid crystalline epoxy resin with spacers outside the mesogenic group. *Molecular Crystals and Liquid Crystals* **609** 80-92.